Tellus SERIES B CHEMICAL AND PHYSICAL METEOROLOGY
PUBLISHED BY THE INTERNATIONAL METEOROLOGICAL INSTITUTE IN STOCKHOLM

Tellus (2009), 61B, 556–565
Printed in Singapore.
TELLUS

Seasonal variation of the molecular hydrogen uptake by soils inferred from continuous atmospheric observations in Heidelberg, southwest Germany

By SAMUEL HAMMER and INGEBORG LEVIN*, *Institut für Umweltphysik, University of Heidelberg, Im Neuenheimer Feld 229, D-69120 Heidelberg, Germany*

(Manuscript received 8 November 2008; in final form 20 February 2009)

ABSTRACT

The dominant sink of atmospheric molecular hydrogen (H_2) is its enzymatic destruction in soils. Quantitative estimates of the global sink strength, as derived from bottom-up process studies, are, however, still associated to large uncertainties. Here we present an alternative way to estimate atmosphere-to-soil flux densities, respectively deposition velocities of H_2, based on atmospheric H_2 and ^{222}Rn observations in the boundary layer. Two and a half years of continuous measurements from a polluted site in the Rhine-Neckar area have been evaluated and night-time flux densities were calculated for situations of strong nocturnal boundary layer inversions using the Radon-Tracer Method. The influences from local anthropogenic combustion sources could be detected and successfully separated by parallel measurements of carbon monoxide. Inferred daily uptake fluxes in the Heidelberg catchment area range from 0.5 to 3 $\times$ 10^{-8} g H_2 m^{-2} s^{-1} with a mean value of (1.28 $\pm$ 0.31) $\times$ 10^{-8} g H_2 m^{-2} s^{-1}. Uptake rates are about 25% larger during summer than during winter, when soil moisture is high, and diffusive transport of H_2 into the soil is inhibited. The mean deposition velocity is 3.0 $\pm$ 0.7 $\times$ 10^{-2} cm s^{-1}, which is very well in line with direct measurements on similar soil types in Europe and elsewhere.

1. Introduction

Molecular hydrogen (H_2) is the second most abundant reduced trace gas in the atmosphere after methane (CH_4), with a global mean mixing ratio of about 500 ppb. The global distribution of H_2 is unique among the major anthropogenically influenced trace gases since H_2 concentrations are lower in the northern than in the southern hemisphere (Novelli et al., 1999; AGAGE, 2007). This points to fundamentally different source distributions compared to all other reactive trace gases in the atmosphere. Two major H_2 source groups can be identified: The first is photochemical H_2 production in the atmosphere; the other are incomplete combustion processes. Photochemical production of H_2 originates from photolysis of formaldehyde (HCHO), a product in the oxidation chain of either CH_4 or other volatile organic compounds (VOCs), and accounts for about half of the global H_2 source. Emissions from incomplete combustion are associated to fossil fuel and biomass burning. Both combustion sources have a similar share in the global H_2 budget ($\approx$15 Tg H_2 yr^{-1}) and together constitute about 40% of the total source. Minor H_2 emissions originate from nitrogen fixation on continents and in the oceans (Novelli et al., 1999; Hauglustaine and Ehhalt, 2002).

The major sinks in the global H_2 cycle are related to H_2 oxidation by hydroxyl free radicals (OH) and the enzymatic H_2 destruction in soils. H_2 oxidation through OH radicals accounts for about 20–30% of the total H_2 sink. At possibly increasing atmospheric H_2 levels the consumption of OH for H_2 oxidation may increase which may result in an increasing lifetime of direct greenhouse gases such as CH_4. The hydrogen peroxy radical (HO_2) produced during atmospheric H_2 oxidation continues to react with nitrogen oxide (NO_x), a key step in photochemical ozone formation (Atkinson, 2000). Oxidation of H_2 in the stratosphere, on the other hand, produces stratospheric water vapour which may imply climatic changes as well as changes in stratospheric chemistry in a future hydrogen economy with elevated atmospheric H_2 mixing ratios (Schultz et al., 2003; Tromp et al., 2003). This is why H_2 is a so-called secondary greenhouse gas (Derwent et al., 2001).

The enzymatic soil uptake of H_2 accounts for about 70–80% of the total global H_2 sink. The underlying processes, including isolation of the enzyme, are not yet completely understood (Guo and Conrad, 2008). Recent studies suggest that the uptake is largely controlled by diffusion in soils, and is, therefore,

*Corresponding author.
e-mail: Ingeborg.Levin@iup.uni-heidelberg.de
DOI: 10.1111/j.1600-0889.2009.00417.x

dependent on soil properties like texture and moisture, besides biological factors (Yonemura et al., 1999; Yonemura et al., 2000b; Schmitt et al., 2009). Still, regional or even global upscaling of parameters controlling the H_2 sink process, the most important component in the global atmospheric H_2 budget, is subject to large uncertainties (Hauglustaine and Ehhalt, 2002; Sanderson et al., 2003) as conclusive process studies and direct flux measurements are still very sparse and do not cover the whole variety of global ecosystems and soils.

However, as will be demonstrated in the present study, at least on the regional scale over continental areas, representative uptake rates can be inferred from atmospheric observations in the boundary layer, as the boundary layer integrates the whole range of source/sink signals in its area of influence. But the challenge lies in disentangling these influence functions. At a continental boundary layer site in Europe, besides signals from the soil sink, large influences from variable local and regional anthropogenic emissions dominate the observed mixing ratios, in addition to the strong modulation of diurnally changing atmospheric transport conditions. In the study presented here we, therefore, measured not only H_2 mixing ratios but also performed continuous observations of other species, namely carbon monoxide (CO) and radon-222 (^{222}Rn), which are used as tracers to separate the influence of anthropogenic emissions (CO) on one hand, and, on the other hand, quantify atmospheric dilution (^{222}Rn). The Radon-Tracer Method (Schmidt et al., 2001) is then applied to the continuous H_2 record to estimate the regional H_2 soil uptake rate in the catchment area of the site (Heidelberg). The particularly strong atmospheric signal from fossil fuel burning sources is evaluated in an accompanying paper by Hammer et al. (2009) where we determine, also in a top-down way, the mean H_2/CO ratio of this source.

2. Methods

2.1. Sampling site

The Heidelberg observational site (49°24′N, 8°42′E, 116 m a.s.l., approximately 130 000 inhabitants) is located in the upper Rhine valley, a semi-polluted region in southwest Germany. Air sampling is installed on the top of the Institut für Umweltphysik building located in the western outskirts of the city. The intake lines, one in the southeastern and one in the southwestern corner of the building are mounted ca. 30 m above local ground. Two different intake lines were used in order to allow detection and elimination of very local contamination (e.g. from the building itself (see below). The Heidelberg sampling site is exposed to a number of local sources: (1) domestic households and traffic from the city, (2) traffic from two highways close by, (3) agricultural land use in the surroundings of the city and (4) densely forested areas further to the east of Heidelberg. An industrial region with sources of numerous trace gases is located about 20 km northwest of the sampling site (Mannheim–Ludwigshafen). Occasionally, direct ‘plumes’ of elevated trace gases from this area are captured in Heidelberg (Schmidt et al., 2001). Large scale biogenic influence is from crop- and grassland in the Rhine valley, but also from the Odenwald, a region of extended forests and grassland at the eastern border of the Rhine valley.

No independent emission statistics for H_2 are available yet for Europe or elsewhere. However, since the production mechanisms for CO and H_2 during combustion processes are very similar (Auckenthaler, 2005), it is generally assumed that the source distribution of anthropogenic H_2 is similar to the one of CO (Novelli et al., 1999). According to this assumption, the major anthropogenic H_2 emissions in the Heidelberg catchment area originate from traffic, while natural H_2 production due to photolysis of HCHO in the troposphere probably only plays a minor role in the short-term variability of H_2. On the other hand, following the global estimates, the soil uptake of H_2, in particular in the Heidelberg catchment area, will be the dominant sink, whereas oxidation in the atmosphere via OH radicals is most probably negligible on time scales of hours to days.

2.2. Experimental techniques

The combined Heidelberg gas chromatographic (GC) system is designed for simultaneous analysis of six trace gases, namely CO_2, CH_4, N_2O, SF_6, CO and H_2. For each trace gas, the GC is optimized to measure ambient concentration levels. The system consists of two commercial GCs, an HP5890II (Hewlett-Packard) and a Reduction Gas Analyser, RGA-3 (Trace Analytics Inc.). These GCs are equipped with three detectors: (1) a Flame Ionization Detector (FID) to analyse CO_2 and CH_4, (2) an Electron Capture Detector (ECD) for N_2O and SF_6 and (3) a Reduction Gas (HgO) Detector for the measurement of CO and H_2. The technical design, the GC parameters used, as well as the applied instrument controls are described in detail by Hammer (2008). Here, we only briefly report on the methods for quasi-continuous atmospheric H_2 and CO mixing ratio measurements and its uncertainties.

From the two permanently flushed intake lines ambient air is collected with two separate membrane pumps (KNF, Neuberger), at a flow rate of 330 ml min^{-1} through a cooling trap at approximately –40 °C, before entering the sample inlet system of the GC. These by-pass lines to the GC are also constantly flushed, while every 5 min a sample is taken either from one of the ambient air lines or from the working gas, and passing through the three sample loops of the three branches of the GC system. The measurement sequence is thus inlet 1, inlet 2 and calibration gas, where at least every 15 min a sample from the southwestern intake line (inlet 1) is analysed. The sample from the southeastern intake line (inlet 2) is missing if other samples such as flasks or further calibration gases are analysed. For the HgO-D branch, which is the last in line with a sample loop volume of 1 ml, we use synthetic air (5.0, hydrocarbon free) as carrier gas. H_2 and CO are separated over a pre-column

[Unibeads 1s, 60–80 Mesh (30 1/4″)] following an analytical column [molecular sieve 5 Å (30 1/4″)], both kept at a temperature of 106 °C, before the sample reaches the HgO detector.

All mixing ratios are calibrated with six primary laboratory standards of concentration ranges between 220 and 822 ppb for H_2 [linked to the EuroHydros 2007 scale (Jordan, 2006)] and between 55 and 900 ppb for CO [linked to the MPI-Mainz scale (Brenninkmeijer et al., 2001)]. For typical atmospheric mixing ratios the reproducibility of individual measurements is ±3 ppb for both gases. The long-term stability of the whole system, checked with a target or surveillance gas which is analysed several times every day, is about 2% for CO and 1.1% for H_2. For data evaluations in this study we calculated half-hourly mean values from the up to four injections performed from the two intake lines within half an hour. Very local contamination from sources in or close to the building would lead to large standard deviations of half-hourly values and respective regression slopes, and are rejected during data evaluation (see Section 3.1).

Atmospheric ^{222}Rn activity is determined via its measured daughter activity using the static filter method (Levin et al., 2002). A disequilibrium factor between atmospheric ^{222}Rn and its daughter polonium-214 of 0.704 was assumed for all measurements.

2.3. *Determination of trace gas fluxes using the Radon-Tracer Method*

The suggestion to use ^{222}Rn as a tracer to parametrize vertical mixing and calculate fluxes of trace gases between soil and atmosphere was first raised by Levin (1984) and has been successfully applied at the Heidelberg sampling station for CH_4 (Levin et al., 1999), N_2O (Schmidt et al., 2001) and fossil fuel CO_2 (Levin et al., 2003). It has been used at other sites, e.g. by Gaudry et al. (1990), Wilson et al. (1997) and Biraud et al. (2000). The fundamental idea of the Radon-Tracer Method is that ^{222}Rn, a noble gas and decay product of natural uranium-238 resp. radium-226, is exhalated from all soils at a rate which, in the catchment area of regional atmospheric observations (10–100 km) varies temporarily by about 30% and spatially, when, e.g. integrated over a square-kilometre, by less than a factor of two (Schüßler, 1996). In the atmosphere the ^{222}Rn activity is solely controlled by radioactive decay and atmospheric mixing.

In a simplified one-dimensional box model approach of the continental boundary layer one can assume that each trace gas released to the atmosphere with a constant rate j accumulates in this well mixed boundary layer of height H at a similar rate. Following Schmidt et al. (2001) the temporal concentration change of ^{222}Rn in this box can be expressed by

$$\frac{dC_{\mathrm{Rn}}}{dt} = \frac{j_{\mathrm{Rn}}}{H(t)} - \lambda_{\mathrm{Rn}} C_{\mathrm{Rn}}. \tag{1}$$

With j_{Rn} being the ^{222}Rn flux density from the soil to the atmosphere and $H(t)$ being the box height which approximates the inversion layer height. The radioactive decay of ^{222}Rn as its ultimate sink has been taken into account by subtracting $\lambda_{\mathrm{Rn}} C_{\mathrm{Rn}}$. For any other (stable) trace gas g emitted or taken up at the soil surface, a similar budget equation can be applied (without a radioactive sink)

$$\frac{dC_g}{dt} = \frac{j_g}{H(t)}. \tag{2}$$

The unknown virtual mixing layer height $H(t)$, considered to be the same for ^{222}Rn and the trace gas g, is eliminated by combining Eq. (1) and (2) and solving for the flux density j_g of the trace gas g. When applying the Rn-Tracer Method, it is reasonable to use finite concentration changes ΔC_g observed, e.g. during one night instead of infinite concentration changes dC_g. This leads to an estimate of the mean trace gas flux density j_g during the observation period Δt of

$$j_g = j_{\mathrm{Rn}} \frac{\Delta C_g}{\Delta C_{\mathrm{Rn}}} \left(1 + \frac{\lambda C_{\mathrm{Rn}}}{\Delta C_{\mathrm{Rn}}/\Delta t}\right)^{-1}. \tag{3}$$

Equation (3) can be simplified, since for short-term variations of $C_{\mathrm{Rn}}(t)$ we can assume that $\lambda_{\mathrm{Rn}} C_{\mathrm{Rn}} \ll \Delta C_{\mathrm{Rn}}/\Delta t$

$$j_g = j_{\mathrm{Rn}} \frac{\Delta C_g}{\Delta C_{\mathrm{Rn}}} \left(1 - \frac{\lambda C_{\mathrm{Rn}}}{\Delta C_{\mathrm{Rn}}/\Delta t}\right). \tag{4}$$

Correction for the radioactive decay of ^{222}Rn in Eq. (4) is taken care of by the term in brackets. During a typical night-time inversion situation, lasting for 5–6 h, the change of ^{222}Rn activity due to radioactive decay is only 3–4%. Therefore, a mean correction factor of 0.965 is applied when estimating ^{222}Rn-based night-time trace gas flux densities (Schmidt et al., 2001). This simple model (which neglects any transport over the box boundary at H, and assumes horizontal homogeneity of the fluxes) is only applicable during relatively stable inversion conditions. Therefore, in this study only nocturnal inversion situations were chosen to investigate temporal concentration changes of H_2 and ^{222}Rn, and derive H_2 flux estimates.

Applying Eq. (4) to estimate trace gas flux densities requires accurate knowledge of the mean ^{222}Rn exhalation rate from the regional ground, including its seasonal variation. Here we use a mean exhalation rate of 56.7 Bq m^{-2} h^{-1} determined by Schüßler (1996) with a seasonal variation of about 30% (Schmidt, 1999). Recent ^{222}Rn source strength estimates using the gamma dose rate as a proxy (Szegvary et al., 2007) fit well to these direct exhalation measurements. For the 0.5° × 0.5° grid box of Heidelberg, Szegvary et al. (2007) estimated an annual mean ^{222}Rn exhalation rate of 55 Bq m^{-2} h^{-1}. This very good agreement may suggest that the uncertainty of the ^{222}Rn exhalation rate we use here is probably less than ±10%.

2.4. *Evaluation of the atmospheric data for estimating night-time H_2 flux densities*

To illustrate the method we used to estimate H_2 soil uptake rates from the 2.5 yr of continuous mixing ratio observations in

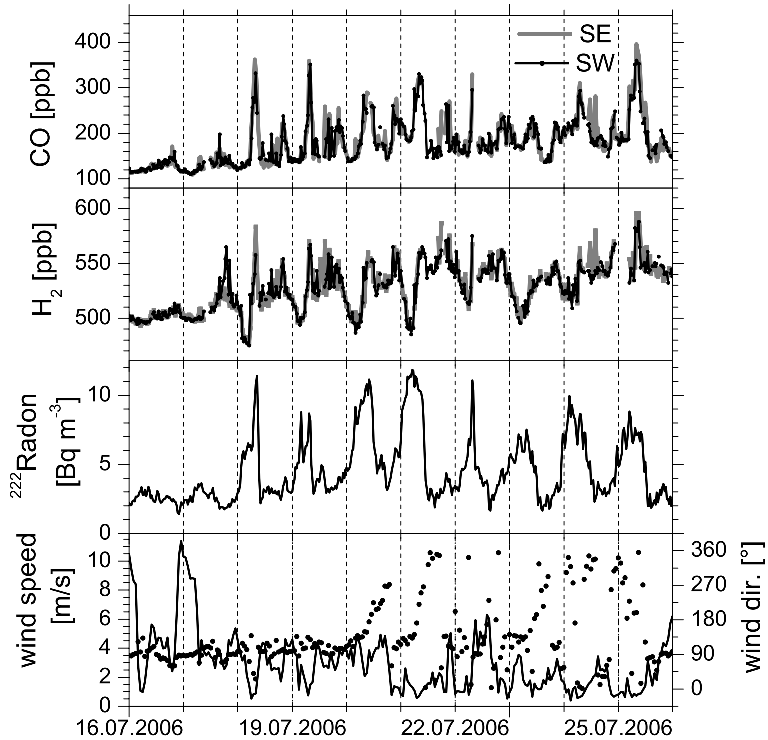

Fig. 1. Typical 10-d record of half-hourly mean mixing ratios of CO, H_2, ^{222}Rn as well as wind speed (solid line) and wind direction (dots). Half-hourly means of CO and H_2 from both intake lines (SE and SW) are shown here.

Heidelberg, a typical 10 d summer record of CO, H_2 and ^{222}Rn measurements as displayed in Fig. 1 is evaluated here in detail. During summer, atmospheric mixing exhibits a regular diurnal pattern: At daytime, strong solar insolation causes large convection, leading to strong vertical mixing and an elevated planetary boundary layer height with generally well-mixed trace gases and only small source or sink signals. Contrary, in clear summer nights the ground cools down rapidly by irradiation. This cooling of the ground causes cooling of the adjacent air layers, and the formation of a so-called nocturnal inversion situation.

During these situations, atmospheric ^{222}Rn, with a more or less constant flux from the ground, slowly increases in the boundary layer, in particular at low wind velocity. The CO record shows a somewhat different behaviour, namely relatively constant low mixing ratios during the night, but sharp spikes during the morning hours and less pronounced peaks in the evenings, attributed to traffic emissions during rush hours. A nocturnal build-up of CO cannot be seen in the data. The missing nocturnal CO build-up indicates the existence of a CO sink, since anthropogenic CO emissions in the Heidelberg catchment area, although largely reduced during night compared to the day, are still significant. The CO sink strength has, thus, to be of the same order as the remaining anthropogenic CO source flux. As the photochemical CO sink is not active during night, soil uptake of CO may be a good candidate for this sink. Enclosure studies performed in the Heidelberg region yield a mean CO soil sink strength of $(2.8 \pm 1.4) \times 10^{-8}$ g CO m^{-2} s^{-1} (Hanselmann, 2008), which is indeed of similar magnitude as anthropogenic night-time CO emissions in the 30 $\times$ 30 km^2 grid around Heidelberg (Institute of Energy Economics and Rational Use of Energy, University of Stuttgart, Germany; personal communication, 2004). The diurnal pattern of H_2 differs again from the two other gases: During stable nocturnal conditions with pronounced increases of ^{222}Rn the H_2 mixing ratio decreases. This decrease is attributed to the presence of the H_2 soil sink. However, in the morning hours, the H_2 mixing ratio increases again a few hours before the nocturnal inversion situation ends. This H_2 increase around 6:00 in the morning is very well in line with the morning spike in CO, and, thus, also attributed to traffic emissions.

By ratioing half-hourly values during the night-time H_2 mixing ratio decrease and the corresponding ^{222}Rn increase, a net H_2 sink strength can be deduced (Eq. 4). However, as for CO, during night time the anthropogenic H_2 sources must still be present, although largely reduced compared to the evening rush hour. Therefore, the net flux density $j_{H_2}^{net}$ of H_2 is the sum of the soil sink and the remaining anthropogenic flux densities:

$$j_{H_2}^{net} = j_{H_2}^{sink} + j_{H_2}^{emi}. \tag{5}$$

The nocturnal H_2 emission flux $j_{H_2}^{emi}$ can be estimated by applying the mean H_2/CO emission ratio of 0.033 g(H_2)/g(CO) (=0.46 mole H_2/mole CO, Hammer et al., 2009) to the nocturnal CO flux, which we assume to be equivalent to the mean CO uptake flux of $(2.8 \pm 1.4) \times 10^{-8}$ g CO m^{-2} s^{-1} (see above). With these assumptions, the mean night-time H_2 emission flux density $j_{H_2}^{emi}$ is, thus estimated to $(0.09 \pm 0.05) \times 10^{-8}$ g H_2 m^{-2} s^{-1}.

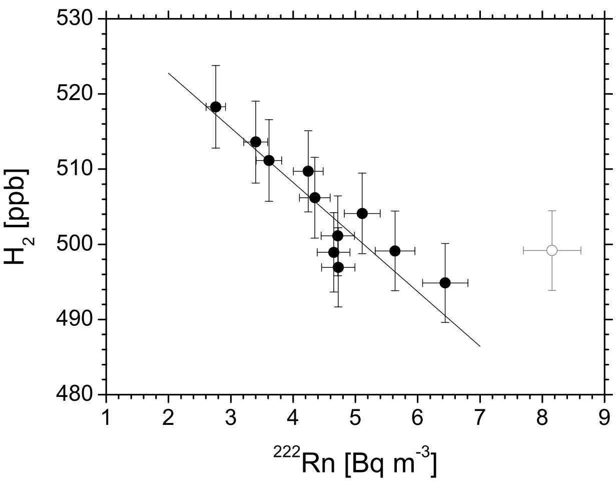

Fig. 2. H_2–^{222}Rn correlation for the night of July 19, 2006 from 0:00 to 5:30 local time, to derive the H_2 soil sink, using Eq. (4). The grey value has been flagged as an outlier.

Applying Eq. (4) with a known ^{222}Rn flux density to the night-time H_2 and ^{222}Rn measurements of Fig. 1 allows individually determining the net H_2 soil sink flux density for each night. Caution is, however, required when selecting the time-span for the nocturnal sink estimate, as the H_2 signal is disturbed by local traffic emissions in the morning rush hours from about 6:00 AM onwards. Also, during the first part of the night (22:00 to 0:00) the H_2 mixing ratios can still be affected by the late evening peak (Fig. 1). Therefore, only the time-span between 0:00 and 5:30 (local time) was selected for the soil sink estimates.

In Fig. 2 the H_2–^{222}Rn correlation is shown for the night of July 19, 2006. While ^{222}Rn accumulates in the boundary layer, the H_2 mixing ratios are depleted. The weighted least-squares algorithm proposed by Krystek and Anton (2007), which accounts for uncertainties in x- and y-direction, yields a slope of (-7.9 ± 1.6) ppb Bq^{-1} m^3. Applying the Radon-Tracer Method (Eq. 4) with a ^{222}Rn flux density of 1.89×10^{-2} Bq m^{-2} s^{-1} valid for July in the Heidelberg catchment area (Schmidt, 1999), and using the slope of the regression line in Fig. 2, an H_2 flux density $j_{H_2} = (-1.4 \pm 0.3) \times 10^{-8}$ g H_2 m^{-2} s^{-1} is obtained. Table 1 shows the values estimated for the individual nights in the summer period shown in Fig. 1. The 1σ errors originate from the uncertainties of the linear fits and represent the statistical error of the Radon-Tracer Method. For the total uncertainty of the ^{222}Rn-based H_2 uptake rates also systematic errors of the ^{222}Rn flux density (which are on the order of 10% in the Heidelberg catchment area, see Section 2.3) have to be considered.

Except for Sunday 23, 2006, the correlation coefficients (R^2) obtained for all nights in Fig. 1 are better than 0.5, showing the generally strong dependence of the H_2 mixing ratio and ^{222}Rn activity changes on atmospheric mixing conditions during the night. In the last two nights the soil flux is significantly smaller than in the previous nights. In the continuous H_2 record (compare Fig. 1) nearly no H_2 draw down is visible for these nights, although the ^{222}Rn levels are comparable to those in the nights before. From our CH_4 and N_2O observations as well as from the wind data we assume that in these nights the continuous Heidelberg measurements were disturbed by local H_2 emissions from the Mannheim–Ludwigshafen industrial region. Thus, disregarding the nights from July 23, 2006 onwards, a mean H_2 soil flux density of $j_{H_2} = (-1.86 \pm 0.47) \times 10^{-8}$ g H_2 m^{-2} s^{-1} is found for July 18–22, 2006. For the whole record, we did, however, only apply criteria on the ^{222}Rn changes as well as on quality of the H_2/^{222}Rn correlation (see Section 3.1), so that occasional influence from the Mannheim–Ludwigshafen industrial region can not be completely excluded.

3. Results

3.1. Data selection and daily mean $\Delta C_{H_2}/\Delta C_{Rn}$ ratios

Quasi-continuous half-hourly atmospheric observations of H_2 mixing ratios and ^{222}Rn activities from January 2005 up until July 2007 have been evaluated in the present study. Since it is mandatory for the Radon-Tracer Method to be applied during stable conditions only, the whole record was first selected for nocturnal inversion situations. The nocturnal ^{222}Rn increase served here as a proxy for the stability of the inversion. Local inversion situations had to be separated from, e.g. synoptic events, as these often go along with a change of the air mass origin. Thus, the concentration decrease/increase during nights with changing synoptic conditions are not only related to surface sources/sinks in the regional catchment area, but also to large-scale catchment area changes. Each selected nocturnal inversion had to fulfil three ^{222}Rn criteria: (1) The absolute ^{222}Rn activity increase rate during the regarded night had to be larger than 1 Bq m^{-3} h^{-1}.

Table 1. H_2 soil flux estimates using the Radon-Tracer Method for 8 d in July 2006 and local night-time periods from 00:00 to 5:30 AM

July 2006	18 Tue	19 Wed	20 Thu	21 Fri	22 Sat	23 Sun	24 Mon	25 Tue
$j_{H_2} \times 10^{-8}$ g H_2 m^{-2} s^{-1}	−1.8	−1.4	−1.5	−2.1	−2.6	−3.9	−0.6	−0.8
1σ	±0.3	±0.3	±0.4	±0.2	±0.7	±1.6	±0.3	±0.6
R^2	0.97	0.89	0.58	0.90	0.70	0.38	0.72	0.51

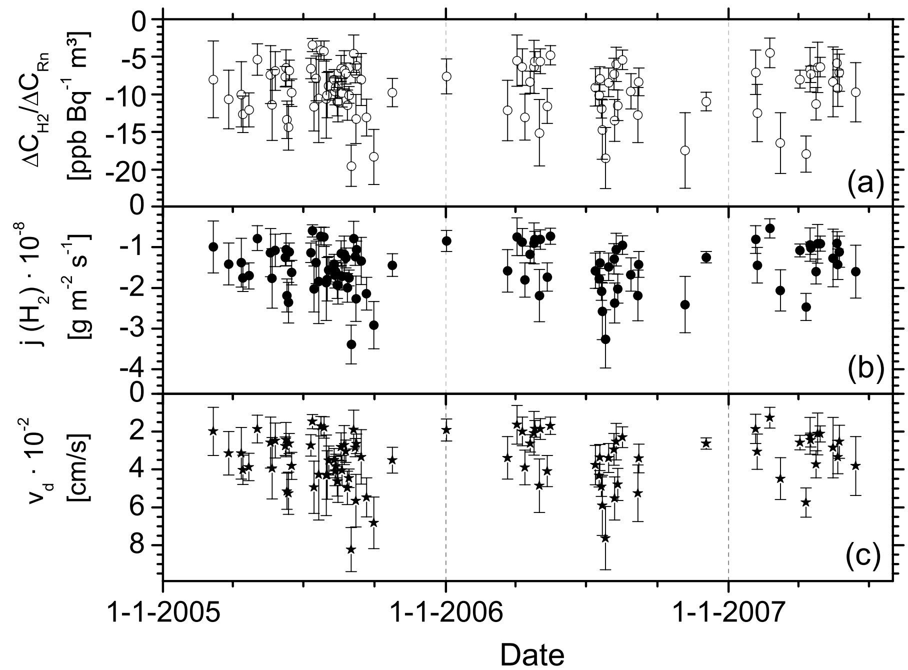

Fig. 3. H_2 soil flux estimates retrieved for days with nocturnal inversion situations. (a) $\Delta C_{H_2}/\Delta C_{Rn}$ ratio retrieved from the correlation in the individual nights. (b) ^{222}Rn-based H_2 flux density j_{H_2}. (c) H_2 deposition velocity v_d calculated according to Eq. (6).

(2) The relative ^{222}Rn increase had to be larger than 40%. (3) The nocturnal ^{222}Rn build-up had to stop between 8:00 and 11:00 in the morning and decrease to ^{222}Rn activities which are comparable to those of the previous day. The last criterion assures that only night-time inversions were included in the H_2 soil sink evaluation. For the period of January 2005 to July 2007, out of 910 nights 151 in total fulfilled all three ^{222}Rn criteria.

For each selected night the H_2 and ^{222}Rn measurements from 0:00 to 5:30 AM (local time) were correlated and, as in Fig. 2, a weighted linear regression function was fit through the data to derive the $\Delta C_{H_2}/\Delta C_{Rn}$ ratio. The retrieved ratio was rejected if the correlation coefficient R^2 was smaller than 0.6, or if the error of the ratio was larger than 50%. After this additional selection, data from 95 nights remained which are shown in Fig. 3a. During the summer months, good data coverage was obtained, but during winter only few data are available. This bias towards spring and summer nights was already visible after the ^{222}Rn criterion which left only less than 15% of the selected nights for the winter (DJF) months. It is caused by the fact that nocturnal inversions occur preferably when the day to night temperature change is large. Thus, the majority of the required strong nocturnal inversion situations occurs during summer. The additional criterion of the quality of the $\Delta C_{H_2}/\Delta C_{Rn}$ correlation ($R^2 > 0.6$) did not cause significant additional bias towards spring and summer values. The data gap in early summer 2006 is caused by missing ^{222}Rn observations. Few nights with potentially good H_2–^{222}Rn correlation but with strong fog are also missing in our record because in these situations, which occur mainly in autumn and winter, we loose ^{222}Rn daughters in the atmosphere, so that the observed correlation with H_2 is bad in those occasions. The observed $\Delta C_{H_2}/\Delta C_{Rn}$ ratios for the selected nights vary between -20 and -3 ppb Bq^{-1} m^3 with a mean $\Delta C_{H_2}/\Delta C_{Rn}$ ratio of -9.5 ppb Bq^{-1} m^3 and a standard deviation of 3.5 ppb Bq^{-1} m^3. No systematic variation (such as a seasonal cycle) is directly visible in the $\Delta C_{H_2}/\Delta C_{Rn}$ ratios. Note that the minimum slope of -3 ppb Bq^{-1} m^3 can be considered as the lower limit where the Radon-Tracer Method could be applied here to estimate H_2 soil uptake rates. It is determined by the measurement accuracy for H_2 mixing ratios and by our criterion, which selects only nights with a ^{222}Rn increase rate larger than 1 Bq m^{-3} h^{-1}. This minimum detected slope translates into a 'detection limit' for the H_2 uptake flux of 0.35×10^{-8} g m^{-2} s^{-1} in winter and 0.52×10^{-8} g m^{-2} s^{-1} in summer. The better detection limit during winter is due to the about 30% smaller ^{222}Rn flux in the winter (DJF) compared to the summer (JJA) months (Schmidt, 1999, cf. Eq. 4). The relatively bad detection limit in winter and the generally small nocturnal ^{222}Rn increases in winter, together with our ^{222}Rn selection criteria, may introduce a bias on the mean winter fluxes towards too high values so that the results presented here should be taken as an upper limit, particularly in winter.

3.2. *Estimates of nocturnal H_2 soil uptake fluxes and respective deposition velocities v_d*

Using Eq. (4) the net H_2 uptake flux density $j_{H_2}^{net}$ was calculated from $\Delta C_{H_2}/\Delta C_{Rn}$ ratios multiplied by the ^{222}Rn flux density j_{Rn}. The monthly mean ^{222}Rn flux density for the Heidelberg catchment area (Schmidt, 1999) was linearly interpolated to daily values. In Fig. 3b the resulting H_2 flux densities are shown. Multiplication of a seasonally varying ^{222}Rn flux density with a peak-to-peak variation of 30% introduces seasonality in the H_2 flux density, which has the same magnitude. Still, a pronounced seasonality of the H_2 flux density with high uptake rates in summer can only be seen in the lower envelope of the data points (Fig. 3b). As mentioned in Section 2.4 only the net H_2 flux density can be obtained from direct atmospheric measurements. Comparing the estimated nocturnal H_2 emission flux of $(0.09 \pm 0.05) \times 10^{-8}$ g m^{-2} s^{-1} (Section 2.4) to the mean net H_2 flux density $j_{H_2}^{net}$ of $(-1.5 \pm 0.6) \times 10^{-8}$ g m^{-2} s^{-1} we can conclude that the nocturnal H_2 emissions have only a minor (6%) influence on the net H_2 flux. Since the estimation of the nocturnal H_2 emission flux is subject to large uncertainties (±50%) we refrain from applying any corrections to the net H_2 uptake flux estimates.

In order to compare our results with other studies, we express the H_2 soil sink strength as H_2 deposition velocity v_d. The H_2 deposition velocity in m/s is defined as the ratio of the mass flux density of H_2 (in g m^{-2} s^{-1}) at the soil surface to the H_2 mass density (in g m^{-3}) in atmospheric air. It can be written as

$$v_d = \frac{j_{H_2}}{\frac{p\, M_{H_2}}{R\, T} C_{H_2}} \tag{6}$$

with the atmospheric pressure p and temperature T, the atmospheric H_2 mixing ratio C_{H_2}, the molar mass of hydrogen M_{H_2} and the gas constant R. For temperature, pressure and H_2 mixing ratio the mean measured values during the nocturnal inversion situations were used.

3.3. *Mean seasonality of the H_2 uptake rate*

In order to investigate the seasonal cycle of the H_2 uptake, the individual H_2 flux densities j_{H_2} resp. the deposition velocities v_d were pooled by month and weighted monthly mean values were calculated which are shown in Fig. 4. Error bars denote the mean uncertainty of each monthly average value. On the top axis, the number of the contributing data points to the monthly mean is given. For j_{H_2} and v_d a fit according to Nakazawa et al. (1997) using two harmonic functions was applied and plotted as a smooth curve through the data. In winter, the data basis is still very sparse, but the slowly increasing soil uptake rate during spring and summer (April–September) is a robust feature of the record. The average values of the first half of this period (April–June) is statistically different from that of the second half (July–September) on a 95% level of confidence. The annual mean H_2 soil flux density j_{H_2} is calculated to $(-1.28 \pm 0.31) \times 10^{-8}$ g H_2 m^{-2} s^{-1} and the respective deposition velocity v_d to $(3.0 \pm 0.7) \times 10^{-2}$ cm s^{-1}. The seasonal cycles have peak-to-peak amplitudes of about 25%. The mean residuals from the fit of the monthly mean deposition velocities are 0.3×10^{-2} cm s^{-1}.

4. Discussion

Table 2 gives an overview of the H_2 soil deposition velocities reported in the literature. For many (bottom-up) chamber studies, only the range of the deposition velocities is given, emphasizing the large temporal variability of the direct soil sink measurements, even on small spatial scales. It is interesting to note that our top-down atmospheric measurements yield very similar ranges of v_d as the chamber studies, and also agree in their maximum uptake rates. As is known from many bottom-up field studies (e.g. Conrad and Seiler, 1985; Yonemura et al., 2000a,b; Schmitt et al., 2009), deposition velocities larger than about 5×10^{-2} cm s^{-1} are only observed on rather dry soils with soil water contents θ_w below 15%. In fact, deposition velocities larger than

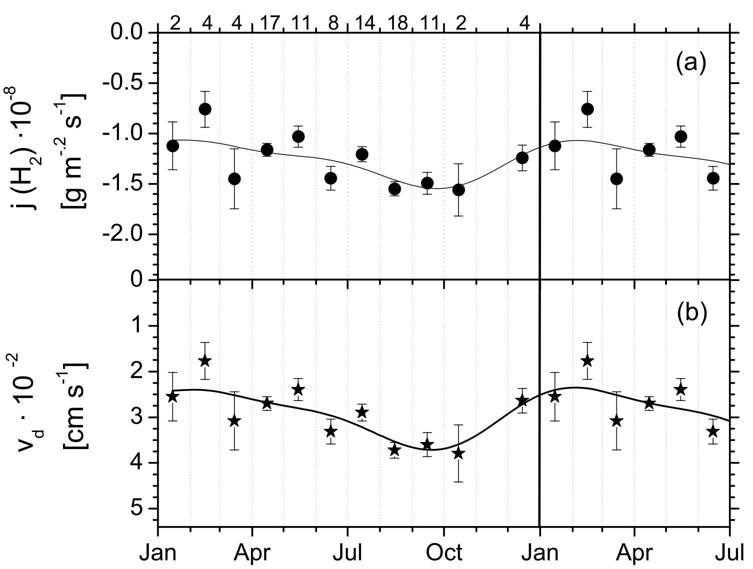

Fig. 4. Mean seasonal cycle of the H_2 soil flux density retrieved from monthly pooled, weighted means of the individual nocturnal flux estimates of Jan. 2005 to July 2007 displayed in Fig. 3b and c. (a) H_2 flux density j_{H_2}, (b) H_2 deposition velocity v_d. For both uptake estimates the number of individual days contributing to the monthly mean is given on the top axis. Error bars denote the mean uncertainty of each monthly mean. Harmonic fit curves are calculated according to Nakazawa et al. (1997).

Table 2. Summary of measured H_2 deposition velocities v_d found in the literature

Authors	Soil type/surrounding	Method	Range $v_d 10^{-2}$ cm s^{-1}	Mean $v_d 10^{-2}$ cm s^{-1}
Conrad and Seiler (1985)	Arid subtropical soil	Chamber	2–13	
Gerst and Quay (2000)	Forest soil	Chamber		4.8 ± 1.3
Yonemura et al. (2000b)	Forest soil	Chamber	5–8	
Yonemura et al. (2000b)	Arable field	Chamber	0–9	
Schmitt et al. (2008)	Arable field	Chamber	1–8	
Simmonds et al. (2000)[a]	Peat soil	Atmospheric		2.6
Rahn et al. (2002)[b]	Burned forest	Atmospheric		4.4 ± 1.3
Rahn et al. (2002)[b]	Mature forest	Atmospheric		7.3 ± 1.5
Steinbacher et al. (2007)[c]	Suburban	Atmospheric	0.5–1	
this study	Urban/suburban	Atmospheric	1–8	3.0 ± 0.7

Note: The investigated soil type or the surroundings and the type of investigation, chamber (bottom-up) or atmospheric (top-down) approach is given. For the atmospheric approaches the respective method is outlined in the footnotes.
[a]Simmonds et al. (2000) used nocturnal ozone depletion to estimate the nocturnal boundary layer height (four nights in May 1996).
[b]Rahn et al. (2002) used chamber measured CO_2 fluxes in combination with the nocturnal $\Delta CO_2/\Delta H_2$ ratio (one week in July 2001).
[c]Steinbacher et al. (2007) calculated the boundary layer height depending on wind speed and temperature (mean boundary layer height 16 m). They use this boundary layer height in combination with a known CO deposition velocity to calculate the H_2 deposition velocity (selected 2.5 yr data set).

5×10^{-2} cm s^{-1} in our top-down study are only observed in summer when soil humidity shows minimum values.

Apart from Steinbacher et al. (2007), all cited studies are based on very limited data, which are often restricted to one season. To our knowledge, the results inferred from atmospheric measurements in Heidelberg are the first estimates, which showed a seasonally varying H_2 uptake rate. For bare soils Schmitt et al. (2009) found a strong dependency of the H_2 soil uptake rate from the soil water content θ_w. It is, therefore, not surprising that the seasonal variation of the H_2 uptake in Heidelberg is also loosely related to the seasonal cycle of the soil moisture in this region (data not shown).

The amplitude of the mean seasonal cycle derived from our observations is small compared to estimates by Hauglustaine and Ehhalt (2002) who report a seasonal variation of the H_2 uptake rate for the Northern Hemisphere changing by a factor of three between summer and winter. Yet one has to keep in mind that Hauglustaine and Ehhalt (2002) assumed that only snow-free soils contribute to the H_2 uptake. From more than 20 yr of satellite observations, Armstrong and Brodzik (2001) derived an annual oscillation of the snow-covered land mass in the Northern Hemisphere of ≈40%, with the smallest snow-cover fraction in late summer. If a seasonal peak-to-peak variation of the soil uptake of 25%, as observed here, is assumed throughout the Northern Hemisphere, and if the seasonal variation in snow-cover is superimposed to this, one can indeed derive an amplitude with a difference of a factor of two between summer and winter.

The seasonal amplitude of the H_2 uptake in our study stems from the seasonality of the ^{222}Rn flux density measured in the Heidelberg catchment area, which is about 30% lower in winter than in summer (Schmidt, 1999). A recent study by Szegvary et al. (2009) reports a seasonal variation of the ^{222}Rn exhalation rate inferred from measured total terrestrial γ-dose rate, which, for our latitude, is only half of what we observe. Applying a smaller seasonality of ^{222}Rn flux to the observed slopes would reduce the seasonality of H_2 uptake by soils accordingly. However, as the ^{222}Rn flux densities used here have been directly measured in our catchment area, we rely on these data rather than on the indirectly determined fluxes reported by Szegvary et al. (2009).

It is worth discussing if one should expect a seasonal variation also in the $\Delta C_{H_2}/\Delta C_{Rn}$ ratio (Fig. 3a). Since both, the ^{222}Rn exhalation rate from soils (e.g. Dörr and Münnich, 1990) as well as the uptake rate of molecular hydrogen in soils are largely diffusion controlled, the ratio of the respective fluxes j_{H_2}/j_{Rn} (which is equal to the concentration slope $\Delta C_{H_2}/\Delta C_{Rn}$, compare Eq. (4)), should, at first order, be not dependent on soil moisture. This is, however, only true, if the diffusion restriction for both gases takes place in the top soil where the variability of soil humidity is also largest.

5. Conclusions

The advantage of the atmospheric top-down approach used here for estimating regional H_2 uptake rates is that it integrates over large spatial scales and soil types. A rough estimate of the catchment area of our measurements can be derived from mean wind velocities during the (calm) nights with strong inversions when we could apply the Radon-Tracer Method. Maximum wind speed under these conditions is 3 m s^{-1}, so that advective flow would carry the signal from a maximum area of about 50 km radius to the sampling site, which would then be equivalent to the maximum area of influence. Also, if enough measurements are available, our method provides reliable and largely representative annual mean values, including profound information on the seasonal cycle. In this study mean H_2 deposition velocities in the range of 2.3–3.7 × 10^{-2} cm s^{-1} were obtained for a Northern Hemispheric mid latitude site. This mean value, although possibly slightly biased towards too high values due to intrinsic limitations of the Radon-Tracer Method, particularly in winter, may be used as a first estimate for Western Europe, respectively areas with similar climatic conditions and soil type distributions as in the Heidelberg region. Particularly encouraging is the very good agreement of our top-down estimate of the H_2 deposition velocity with bottom-up results from direct chamber measurements. Extending the method proposed and applied in this study to other continental sites will largely help to better quantify the most important component of the atmospheric molecular Hydrogen budget.

6. Acknowledgments

We wish to thank Christel Facklam and Michael Sabasch for their help in continuous atmospheric H_2 and CO measurements, and Felix Vogel for many fruitful discussions. The RGA-3 instrument used in this study was kindly made available to us by Andreas Volz-Thomas, Forschungszentrum Jülich, Germany. This work was partially funded by the European Union under projects No. GOCE-CT2003-505572 (CarboEurope-IP) and No. FP6-2005-Global4-03916 (EuroHydros).

References

AGAGE. 2007. Advanced global atmospheric gases experiment (AGAGE), database. Online at: www.agage.eas.gatech.edu/data.htm.

Armstrong, R. L. and Brodzik, M. J. 2001. Recent Northern Hemisphere snow extent: a comparison of data derived from visible and microwave satellite sensors. *Geophys. Res. Lett.* **28**, 3673–3676.

Atkinson, R. 2000. Atmospheric chemistry of VOCs and NOx. *Atmos. Environ.* **34**(12–14), 2063–2101.

Auckenthaler, T. S. 2005. *Modelling and Control of Three-way Catalytic Converters*. PhD Thesis. Swiss Federal Institute of Technology, Zürich, Switzerland, Thesis, No. 16018.

Biraud, S., Ciais, P., Ramonet, M., Simmonds, P. Kazan, V. and co-authors. 2000. European greenhouse gas emissions estimated from continuous atmospheric measurements and radon 222 at Mace Head, Ireland. *J. Geophys. Res.* **105**(D1), 1351–1366.

Brenninkmeijer, C. A. M., Koeppel, C., Röckmann, T., Scharffe, D. S., Bräunlich, M. and co-authors. 2001. Absolute measurement of the abundance of atmospheric carbon monoxide. *J. Geophys. Res.* **106**, 10,003–10,010.

Conrad, R. and Seiler, W. 1985. Influence of temperature, moisture, and organic carbon on the flux of H_2 and CO between soil and atmosphere: field studies in subtropical regions. *J. Geophys. Res.* **90**, 5699–5709.

Derwent, R. G., Collins, W. J., Johnson, C. E. and Stevenson, D. S. 2001. Transient behaviour of tropospheric ozone precursors in a global 3-D CTM and their indirect greenhouse effects. *Clim. Change* **49**, 463–487.

Dörr, H. and Münnich, K. O. 1990. ^{222}Rn flux and soil air concentration profiles in West-Germany. Soil ^{222}Rn as tracer for gas transport in the unsaturated soil zone. *Tellus* **42B**, 20–28.

Gaudry, A., Polian, G., Ardouin, B. and Lambert, G. 1990. Radon-calibrated emissions of CO_2 from South Africa. *Tellus* **42B**, 9–19.

Gerst, S. and Quay, P. 2000. The deuterium content of atmospheric molecular hydrogen: method and initial measurements. *J. Geophys. Res.* **105**, 26433–26446.

Guo, R. and Conrad, R. 2008. Extraction and characterization of soil hydrogenases oxidizing atmospheric hydrogen. *Soil Biol. Biochem.* **40**(5), 1149–1154.

Hammer, S. 2008. *Quantification of the Regional H_2 Sources and Sinks Inferred from Atmospheric Trace Gas Variability*. PhD Thesis. University of Heidelberg, Germany.

Hammer, S., Vogel, F., Kaul, M. and Levin, I. 2009. The H_2/CO ratio of emissions from combustion sources: comparison of top-down with bottom-up measurements in the Rhine-Neckar region in south-west Germany. *Tellus* **61B**, doi:10.1111/j.1600-0889.2009.00418.x.

Hanselmann, A. 2008. *Field Study to Assess Uptake and Emission of Trace Gases from Soils*. Diploma Thesis, Institut für Umweltphysik, University of Heidelberg, Germany.

Hauglustaine, D. A. and Ehhalt, D. H. 2002. A three-dimensional model of molecular hydrogen in the troposphere. *J. Geophys. Res.* **107**, D17, 4330 ACH41-16.

Jordan, A. 2006. *Calibration of Atmospheric Hydrogen, Proceedings of the13th WMO/IAEA Meeting of Experts on Carbon Dioxide Concentration and Related Tracers Measurement Techniques*. Boulder, Colorado, USA, 19–22 September 2005. (WMO TD No. 1359).

Krystek, M. and Anton, M. 2007. A weighted total least-squares algorithm for fitting a straight line. *Measure. Sci. Technol.* **18**, 3438–3442.

Levin, I. 1984. *Atmosphärisches CO_2, Quellen und Senken auf dem Europäischen Kontinent*. PhD Thesis. University of Heidelberg, Germany.

Levin, I., Glatzel-Mattheier, H., Marik, T., Cuntz, M., Schmidt, M. and co-authors. 1999. Verification of German methane emission inventories and their recent changes based on atmospheric observations. *J. Geophys. Res.* **104**(D3), 3447–3456.

Levin, I., Born, M., Cuntz, M., Langendörfer, U., Mantsch, S. and co-authors. 2002. Observations of atmospheric variability and soil exhalation rate of Radon-222 at a Russian forest site: technical approach and deployment for boundary layer studies. *Tellus* **54B**, 462–475.

Levin, I., Kromer, B., Schmidt, M. and Sartorius, H. 2003. A novel approach for independent budgeting of fossil fuels CO_2 over Europe by $^{14}CO_2$ observations. *Geophys. Res. Lett.* **30**(23), 2194, doi: 10.1029/2003GL018477.

Nakazawa, T., Ishizawa, M., Higuchi, K. and Trivett, N. 1997. Two curve fitting methods applied to CO_2 flask data. *Environ. Metrics* **8**, 197–218.

Novelli, P. C., Lang, P. M., Masarie, K. A., Hurst, D. F., Myers, R. and co-authors. 1999. Molecular hydrogen in the troposphere: global distribution and budget. *J. Geophys. Res.* **104**, 30427–30444.

Rahn, T., Eiler, J. M., Kitchen, N., Fessenden, J. E. and Randerson, J. T. 2002. Concentration and δD of molecular hydrogen in boreal forests: ecosystem-scale systematics of atmospheric H_2. *Geophys. Res. Lett.* **29**, 35–1.

Sanderson, M., Collins, W., Derwent, R. and Johnson, C. 2003. Simulation of global hydrogen levels using a lagrangian three-dimensional model. *J. Atmos. Chem.* **46**, 15–28.

Schmidt, M. 1999. *Messung und Bilanzierung anthropogener Treibhausgase in Deutschland*. PhD Thesis. University of Heidelberg, Germany.

Schmidt, M., Glatzel-Mattheier, H., Sartorious, H., Worthy, D. E. and Levin, I. 2001. Western European N_2O emissions: a top-down approach based on atmospheric observations. *J. Geophys. Res.* **106**(D6), 5507–5516.

Schmitt, S., Hanselmann, A., Wollschläger, U., Hammer, S. and Levin, I. 2009. Investigation of parameters controlling the soil sink of atmospheric molecular hydrogen. *Tellus* **61B**, 416–423.

Schüßler, W. 1996. *Effektive Parameter zur Bestimmung des Gasaustauschs zwischen Boden und Atmosphäre*. PhD Thesis. University of Heidelberg, Germany.

Schultz, M. G., Diehl, T., Brasseur, G. P. and Zittel, W. 2003. Air pollution and climate-forcing impacts of a global hydrogen economy. *Science* **302**, 624–627.

Simmonds, P. G., Derwent, R. G., O'Doherty, S., Ryall, D. B., Steele, L. P. and co-authors. 2000. Continuous high-frequency observations of hydrogen at the Mace Head baseline atmospheric monitoring station over the 1994–1998 period. *J. Geophys. Res.* **105**, 12105–12122.

Steinbacher, M., Fischer, A., Vollmer, M. K., Buchmann, B., Reimann, S. and co-authors. 2007. Perennial observations of molecular hydrogen (H_2) at a suburban site in Switzerland. *Atmos. Environ.* **41**(10), 2111–2124.

Szegvary, T., Leuenberger, M. C. and Conen, F. 2007. Predicting terrestrial ^{222}Rn flux using gamma dose rate as a proxy. *Atmos. Chem. Phys.* **7**(11), 2789–2795 (available online: http://radon.unibas.ch).

Szegvary, T., Conen, F. and Ciais, P. 2009. European ^{222}Rn inventory for applied atmospheric studies. *Atmos. Environ.* doi: 10.1016/j.atmosenv.2008.11.025.

Tromp, T. K., Shia, R. L., Allen, M. and Eiler, J. M. 2003. Potential environmental impact of a hydrogen economy on the stratosphere. *Science* **300**, 1740–1742.

Wilson, S. R., Dick, A. L., Fraser, P. J. and Whittlestone, S. 1997. Nitrous oxide flux estimates for south-eastern Australia. *J. Atmos. Chem.* **26**, 169–188.

Yonemura, S., Yokozawa, M., Kawashima, S. and Tsuruta, H. 1999. Continuous measurements of CO and H_2 deposition velocities onto an andisol: uptake control by soil moisture. *Tellus* **51B**, 688–700.

Yonemura, S., Kawashima, S. and Tsuruta, H. 2000a. Carbon monoxide, hydrogen, and methane uptake by soils in a temperate arable field and a forest. *J. Geophys. Res.* **105**, 347–362.

Yonemura, S., Yokozawa, M., Kawashima, S. and Tsuruta, H. 2000b. Model analysis of the influence of gas diffusivity in soil and on CO and H_2 uptake. *Tellus* **52B**, 919–933.